



This is a repository copy of *Tracking of wireless mobile nodes in he presence of unknown path-loss characteristics*.

White Rose Research Online URL for this paper:

<https://eprints.whiterose.ac.uk/91862/>

Version: Accepted Version

Proceedings Paper:

Khan, M.W., Kemp, A.H., Salman, N. et al. (1 more author) (2015) Tracking of wireless mobile nodes in he presence of unknown path-loss characteristics. In: 18th International Conference on Information Fusion (Fusion). 18th International Conference on Information Fusion, 06-09 Jul 2015, Washington, DC. IEEE , 104 - 111 .

Reuse

Items deposited in White Rose Research Online are protected by copyright, with all rights reserved unless indicated otherwise. They may be downloaded and/or printed for private study, or other acts as permitted by national copyright laws. The publisher or other rights holders may allow further reproduction and re-use of the full text version. This is indicated by the licence information on the White Rose Research Online record for the item.

Takedown

If you consider content in White Rose Research Online to be in breach of UK law, please notify us by emailing eprints@whiterose.ac.uk including the URL of the record and the reason for the withdrawal request.



eprints@whiterose.ac.uk
<https://eprints.whiterose.ac.uk/>

Tracking of Wireless Mobile Nodes in the Presence of Unknown Path-loss Characteristics

M. W. Khan and A. H. Kemp

School of Electronic and Electrical Engineering
University of Leeds, UK
Email: {elmwk, a.h.kemp}@leeds.ac.uk

N. Salman and L. S. Mihaylova

Department of Automatic Control and Systems Engineering
University of Sheffield, UK
Email: {n.salman, l.s.mihaylova}@sheffield.ac.uk

Abstract—Due to the difficult characterization of the propagation model, most studies on tracking of mobile nodes assume the correct knowledge of the power-distance gradients or the path-loss exponents (PLEs). In this paper, we first investigate the impact of erroneous PLEs on positioning of a wireless nodes when both distance and bearing measurements are available. Thus, an analytical expression of the mean square error (MSE) in location estimation is derived in case of erroneous PLEs. Second, we propose a novel online PLE estimation and tracking algorithm in dynamic environments. The proposed algorithm estimates the PLE of individual links at every time-step using the generalized pattern search (GenPS) algorithm. The PLE estimates update the observation vector which is used in a Kalman filter (KF) and a particle filter (PF) for tracking. Simulation results show that the tracking performance degrades drastically with an incorrect assumption for the PLE values. Further simulations show that tracking with PLE estimation performs considerably better compared to tracking with incorrectly assumed PLEs.

I. INTRODUCTION

Mobile target tracking is an important research topic that has become essential for many new applications. The observations from fixed sensor nodes (SNs) with known locations can be used for bearing and distance estimation. The simplest technique for distance estimation is the received signal strength (RSS) technique as no additional hardware is required. The accuracy of the location estimate via RSS is highly dependent on knowledge of the path loss exponents (PLEs) of individual target node (TN) to SN links. Indeed, the PLE value for free space is two. However in highly cluttered environments this value could range from two-five [1]. The assumption of having the correct information about PLEs is an oversimplification. Practically this information is not available, especially in uncertain propagation environments. One way to estimate the PLE is via an offline measurement campaign. This however is impractical in dynamic environments i.e., environments in which the PLEs change constantly in time e.g., due to mobility of the TN. Some recent studies jointly estimate the location coordinates and the PLE for localization [2], [3], [4] for RSS observations only. However, these studies assume the same PLE value for every SN-TN link, this again is an oversimplification of real conditions. In this paper, we assume unknown and different PLEs for each SN-TN link. We use a hybrid angle of arrival-received signal strength (AoA-RSS) signal model, presented in our previous work in [5]. The angle of arrival of the received signal can be estimated by

a rotating beam of radiation [6] or by using a multi-element array antenna [7] and using techniques such as Multiple Signal Classification (MUSIC) [8] or estimation of signal parameters via rotational invariance techniques (ESPIRT) [9].

In order to underline the impact of incorrect PLE assumption on location estimates, we first derive a closed form expression of the mean square error (MSE) of location estimates with different and incorrect PLE values. Secondly, we propose an online joint PLE and tracking technique when both bearing and RSS measurements are available. This is achieved by modifying the observation model into a multivariable optimization problem and then applying the generalized pattern search (GenPS) algorithm to estimate the PLEs. The estimated PLEs are assumed to be changing at every time step and tracking is performed via a Kalman filter (KF) [10] and a particle filter (PF) [11]. Although, the observations are linearized before filtering, the noise in the linearized observation does not remain Gaussian. Extensive simulations are performed to compare the performance of both filters with inaccurate PLE assumption and with estimated PLEs. It is shown via simulations that the online PLE estimation considerably improves the tracking performance of both KF and PF. However, due to the non-Gaussian nature of the linearized observation model the PF outperforms the KF.

The rest of the paper is organized as follows: Section II presents the linearized hybrid AoA-RSS signal model. In section III, we derive the MSE expression on location estimation for incorrect PLEs. In section IV, we present the tracking algorithms. PLE estimation via the GenPS algorithm is presented in section V. Finally simulation results are discussed in section VI which are followed by conclusion in section VII.

II. THE LINEARIZED HYBRID AOA-RSS SIGNAL MODEL

In this section the linearized AoA-RSS signal model is briefly reviewed.

For later use, we define the following notations. \mathbb{R}^n represents the set of n dimensional real numbers; \mathbb{Z}^n represents the set of integers of dimension n ; $\| \cdot \|$ represents the Euclidean norm; $tr(\mathbf{M})$ represents the trace of the matrix \mathbf{M} ; $(\cdot)^T$ represents the transpose operation; $E_n(\cdot)$ represents the expectation operation with respect to n ; $(\mathbf{M})_{ij}$ represents the element at the i^{th} row and j^{th} column of matrix \mathbf{M} ; \mathbf{I}_n is the

identity matrix of dimension n ; $\mathcal{N}(\mu, \sigma^2)$ denotes the normal distribution with mean μ and variance σ^2 ; $\mathcal{U}[a, b]$ represents a uniform distribution between a and b .

With both distance and angle measurements at hand, the coordinates of the TN at the t^{th} time step can be computed as follows

$$\hat{x}_t = \bar{x}_i + \hat{d}_{it} \cos \hat{\theta}_{it} \delta_i, \quad (1)$$

$$\hat{y}_t = \bar{y}_i + \hat{d}_{it} \sin \hat{\theta}_{it} \delta_i, \quad (2)$$

where \bar{x}_i, \bar{y}_i are the coordinates of the SNs for $i = 1, \dots, N$. The estimated distance \hat{d}_{it} can be readily extracted from the received path-loss at the i^{th} SN at time-step t , \mathcal{L}_{it} .

$$\mathcal{L}_{it} = \mathcal{L}_0 + 10\alpha_{it} \log_{10} d_{it} + n_{it}, \quad (3)$$

For ease of understanding we will drop the subscript t . In (3), \mathcal{L}_0 is the path loss at reference distance d_0 , normally taken as 1m. α_i is the PLE associated with i^{th} SN. $d_i = \sqrt{(\bar{x}_i - x)^2 + (\bar{y}_i - y)^2}$, n_i is the zero mean Gaussian random variable representing the log-normal shadowing i.e., $n_i \sim \mathcal{N}(0, \sigma_{n_i}^2)$. The path-loss is the difference between the transmit power P at the TN and the received power P_i at the i^{th} SN and is given by

$$\mathcal{L}_i = 10 \log_{10} P - 10 \log_{10} P_i. \quad (4)$$

The observed path-loss \hat{z}_i from d_0 to d_i is given by $\mathcal{L}_i - \mathcal{L}_0$, and can be represented as

$$\hat{z}_i = \gamma \alpha_i \ln d_i + n_i, \quad (5)$$

for $\gamma = \frac{10}{\ln 10}$. To obtain the unbiased distance estimate from the observed path-loss, (5) can be written as

$$\hat{d}_i = d_i \exp\left(\frac{n_i}{\gamma \alpha_i}\right) \kappa_i, \quad (6)$$

where κ_i is the unbiasing constant for range estimate and is given by

$$\kappa_i = \exp\left(-\frac{\sigma_{n_i}^2}{2(\gamma \alpha_i)^2}\right). \quad (7)$$

On the other hand, the estimated angle of arrival $\hat{\theta}_i$ of the impinging signal is given by

$$\hat{\theta}_i = \arctan\left(\frac{(y - \bar{y}_i)}{(x - \bar{x}_i)}\right) + m_i, \quad (8)$$

where m_i is the zero mean Gaussian random variable representing the noise in angle estimate i.e., $m_i \sim \mathcal{N}(0, \sigma_{m_i}^2)$. With the above observations, (1) and (2) can be written in a vector form as

$$\mathbf{u} = \mathbf{A}^\dagger \hat{\mathbf{b}}, \quad (9)$$

where $\mathbf{u} = [\hat{x} \ \hat{y}]^T$ is the TN coordinates, \mathbf{A}^\dagger is the Moore–Penrose pseudo-inverse of \mathbf{A} and $\mathbf{A} = \text{diag}(\mathbf{e}_1, \mathbf{e}_1)$ where \mathbf{e}_1 is a column vector of N ones. The observation matrix $\hat{\mathbf{b}}$ is given by

$$\hat{\mathbf{b}} = \begin{bmatrix} \hat{\mathbf{b}}_x & \hat{\mathbf{b}}_y \end{bmatrix}^T, \quad (10)$$

$$\hat{\mathbf{b}}_x = \begin{bmatrix} x_1 + \hat{d}_1 \cos \hat{\theta}_1 \delta_1 \\ \vdots \\ x_N + \hat{d}_N \cos \hat{\theta}_N \delta_N \end{bmatrix}, \hat{\mathbf{b}}_y = \begin{bmatrix} y_1 + \hat{d}_1 \sin \hat{\theta}_1 \delta_1 \\ \vdots \\ y_N + \hat{d}_N \sin \hat{\theta}_N \delta_N \end{bmatrix},$$

where δ_i is the unbiasing constant for the hybrid AoA-RSS signal and is given by

$$\delta_i = \kappa_i \rho_i, \quad (11)$$

where ρ_i is the unbiasing constant for angle estimate given by

$$\rho_i = \exp\left(\frac{\sigma_{m_i}^2}{2}\right).$$

III. THEORETICAL MSE FOR ERRONEOUS PLES

In this section, we derive the theoretical MSE to observe the impact of incorrect PLE assumption on location estimation. First we use the observed path-loss (5) to extract the range between SN and TN when the true values of PLEs are not known. Using the erroneous PLE values we have from (5)

$$\frac{z_i}{\gamma \check{\alpha}_i} = \frac{\alpha_i}{\check{\alpha}_i} \ln d_i + \frac{n_i}{\gamma \check{\alpha}_i}, \quad (12)$$

where $\check{\alpha}_i$ is the incorrect PLE for the i^{th} SN i.e., $\check{\alpha}_i = \alpha_i + e_i$, and e_i represents the error in PLE associated with i^{th} SN. Taking exponential on both side of (12), the unbiased distance estimate using and erroneous PLE is obtained as

$$\check{d}_i = d_i^{\beta_i} \exp\left(\frac{n_i}{\gamma \check{\alpha}_i}\right) \Lambda_i, \quad (13)$$

where $\beta_i = \alpha_i / \check{\alpha}_i$ and $\Lambda_i = \exp\left(-\frac{\sigma_{n_i}^2}{2(\gamma \check{\alpha}_i)^2}\right)$.

For the aforementioned hybrid AoA-RSS signal model, (13) is taken as the distance estimate in (10) i.e., we use \check{d}_i instead of \hat{d}_i . Also the unbiasing constant δ_i is changed to $\check{\delta}_i = \Lambda_i \rho_i$. The theoretical MSE is then given by [12]

$$\text{MSE} = \text{tr} \left\{ E_{n,m} \left[(\check{\mathbf{u}} - \mathbf{u})(\check{\mathbf{u}} - \mathbf{u})^T \right] \right\}, \quad (14)$$

where $\check{\mathbf{u}}$ is the estimated location using noisy angle estimates and noisy range estimates and incorrect PLEs, while \mathbf{u} is the location with no noise and correct PLE values. Thus (14) can be simplified to

$$\text{MSE}(\mathbf{u}) = \mathbf{A}^\dagger \mathbf{C}_\alpha(\mathbf{u}) \mathbf{A}^{\dagger T}, \quad (15)$$

where $\mathbf{C}_\alpha(\mathbf{u}) = E_{n,m} \left[(\check{\mathbf{b}} - \mathbf{b})(\check{\mathbf{b}} - \mathbf{b})^T \right]$, for \mathbf{b} representing the noise-free observation, $\check{\mathbf{b}}$ representing the noisy observation and incorrect PLEs and $E_{n,m}$ is the expectation w.r.t. shadowing and noise associated with angle estimates. The covariance $\mathbf{C}_\alpha(\mathbf{u})$ can be partitioned into separate submatrices as follows

$$\mathbf{C}_\alpha(\mathbf{u}) = \begin{bmatrix} \mathbf{C}_\alpha(x) & \mathbf{C}_\alpha(xy) \\ \mathbf{C}_\alpha(xy) & \mathbf{C}_\alpha(y) \end{bmatrix}. \quad (16)$$

$\mathbf{C}_\alpha(x)$, $\mathbf{C}_\alpha(y)$ and $\mathbf{C}_\alpha(xy)$ reduces to (17), (18) and (19), respectively, for $i = j$ and (20), (21) and (22), respectively for $i \neq j$. Derivation is given in the Appendix.

$$\mathbf{C}_\alpha(x)_{ii} = d_i^{2\beta_i} \left(\frac{\sigma_{n_i}^2}{(\gamma\check{\alpha}_i)^2} + \sigma_{m_i}^2 \right) + \frac{d_i^{2\beta_i}}{2} \cos(2\theta_i) \exp \left(\frac{\sigma_{n_i}^2}{(\gamma\check{\alpha}_i)^2} - \sigma_{m_i}^2 \right) + (d_i \cos \theta_i)^2 - 2d_i d_i^{\beta_i} \cos^2 \theta_i \quad (17)$$

$$\mathbf{C}_\alpha(y)_{ii} = d_i^{2\beta_i} \left(\frac{\sigma_{n_i}^2}{(\gamma\check{\alpha}_i)^2} + \sigma_{m_i}^2 \right) - \frac{d_i^{2\beta_i}}{2} \cos(2\theta_i) \exp \left(\frac{\sigma_{n_i}^2}{(\gamma\check{\alpha}_i)^2} - \sigma_{m_i}^2 \right) + (d_i \sin \theta_i)^2 - 2d_i d_i^{\beta_i} \sin^2 \theta_i \quad (18)$$

$$\mathbf{C}_\alpha(xy)_{ii} = d_i^{2\beta_i} \cos \theta_i \sin \theta_i \exp \left(\frac{\sigma_{n_i}^2}{(\gamma\check{\alpha}_i)^2} - \sigma_{m_i}^2 \right) - 2d_i^{\beta_i} \cos \theta_i \sin \theta_i + d_i^2 \cos \theta_i \sin \theta_i \quad (19)$$

$$\mathbf{C}_\alpha(x)_{ij} = \left(d_i^{\beta_i} d_j^{\beta_j} - d_i^{\beta_i} d_j - d_i d_j^{\beta_j} + d_i d_j \right) \cos \theta_i \cos \theta_j \quad (20)$$

$$\mathbf{C}_\alpha(y)_{ij} = \left(d_i^{\beta_i} d_j^{\beta_j} - d_i^{\beta_i} d_j - d_i d_j^{\beta_j} + d_i d_j \right) \sin \theta_i \sin \theta_j \quad (21)$$

$$\mathbf{C}_\alpha(xy)_{ij} = \left(d_i^{\beta_i} d_j^{\beta_j} - d_i^{\beta_i} d_j - d_i d_j^{\beta_j} + d_i d_j \right) \cos \theta_i \sin \theta_j \quad (22)$$

IV. TARGET TRACKING

A target moving in a two dimensional field can be described by its position and velocity in the x, y plane. Numerous motion models are proposed in the literature, these include random walk model, the constant velocity model and Singer types models [13]. In this paper, we consider the basic constant velocity model to describe the motion of the TN. Both the KF and PF consist of the prediction and the measurement step.

A. Prediction Step

The motion of the TN in a network is represented by the state equation

$$\bar{\mathbf{v}}_t = \mathbf{S}\hat{\mathbf{v}}_{t-1} + \mathbf{r}_t, \quad (23)$$

where \mathbf{S} is the transition matrix given by

$$\mathbf{S} = \begin{bmatrix} 1 & 0 & T_s & 0 \\ 0 & 1 & 0 & T_s \\ 0 & 0 & 1 & 0 \\ 0 & 0 & 0 & 1 \end{bmatrix}. \quad (24)$$

$\bar{\mathbf{v}}_t = [x_t, y_t, v_x, v_y]^T$ is the state vector, where x and y are the coordinates, v_x and v_y are the velocities in x and y direction respectively at time step t . $\hat{\mathbf{v}}_{t-1}$ is the output of measurement step at time step $t-1$; \mathbf{r}_t represents the process noise, which we assumed to be a zero mean Gaussian white noise with covariance \mathbf{Q}_t i.e., $\mathbf{r}_t \sim \mathcal{N}(0, \mathbf{Q}_t)$. T_s is the sampling time interval between two consecutive time steps.

B. Measurement Step

Measurements at the SNs are represented by

$$\hat{\mathbf{b}}_t = \mathbf{H}\bar{\mathbf{v}}_t + \mathbf{c}_t. \quad (25)$$

For an AoA-RSS signal model, $\mathbf{H} = [\text{diag}(\mathbf{e}_1, \mathbf{e}_1), \text{diag}(\mathbf{e}_0, \mathbf{e}_0)]$, \mathbf{e}_1 and \mathbf{e}_0 are the column vectors of N ones and N zeros, respectively and

$$\hat{\mathbf{b}}_t = \begin{bmatrix} x_1 + \hat{d}_{1t} \cos \hat{\theta}_{1t} \delta_1, \dots, x_N + \hat{d}_{Nt} \cos \hat{\theta}_{Nt} \delta_N \\ y_1 + \hat{d}_{1t} \sin \hat{\theta}_{1t} \delta_1, \dots, y_N + \hat{d}_{Nt} \sin \hat{\theta}_{Nt} \delta_N \end{bmatrix}^T \quad (26)$$

which is the same observation matrix as (10). Thus \hat{d}_{it} , $\hat{\theta}_{it}$ are the distance and angle estimates respectively at time step t . \mathbf{c}_t represents the measurement noise with zero mean and covariance \mathbf{C}_t , given by

$$\mathbf{C}_t = \begin{bmatrix} \mathbf{C}_t(x) & \mathbf{C}_t(xy) \\ \mathbf{C}_t(xy) & \mathbf{C}_t(y) \end{bmatrix}, \quad (27)$$

$\mathbf{C}_t(x)$, $\mathbf{C}_t(y)$ and $\mathbf{C}_t(xy)$ are given by (32), (33) and (34), respectively for $i = j$ and their values are zero for $i \neq j$, and are derived by the authors in [5]. In the measurement step, the output of the predicted step is refined by exploiting the observations $\hat{\mathbf{b}}_t$ and the covariance \mathbf{C}_t .

C. Kalman Filter

The KF is one of the most important and common data fusion algorithms in use today. The KF uses the fact that the state of the system at time t is evolved from the prior state at time $t-1$ according to (23). In the prediction step, starting from the initial state $\hat{\mathbf{v}}_0$ and initial error covariance matrix \mathbf{W}_0 , the KF propagates and updates $\hat{\mathbf{v}}_0$ according to (23) and \mathbf{W}_0 according to (28) at each time step.

$$\bar{\mathbf{W}}_t = \mathbf{S}\mathbf{W}_{t-1}\mathbf{S}^T + \mathbf{Q}_t. \quad (28)$$

The measurement step is also two fold, the Kalman gain is calculated using

$$\mathbf{K}_t = \bar{\mathbf{W}}_t \mathbf{H}^T (\mathbf{H} \bar{\mathbf{W}}_t \mathbf{H}^T + \mathbf{C}_t). \quad (29)$$

Once the Kalman gain is calculated, the estimates from predictions step are updated using

$$\hat{\mathbf{v}}_t = \bar{\mathbf{v}}_t + \mathbf{K}_t (\hat{\mathbf{b}}_t - \mathbf{H}\bar{\mathbf{v}}_t) \quad (30)$$

and

$$\mathbf{W}_t = (\mathbf{I}_4 - \mathbf{K}_t \mathbf{H}) \bar{\mathbf{W}}_t, \quad (31)$$

where \mathbf{I}_4 is a 4×4 identity matrix. Equation (31) becomes the input for the prediction step at time step $t+1$.

The KF is an optimal estimator when the observation model is linear and all noises are Gaussianly distributed. In case of nonlinear models several variants of KF like extended KF (EKF) and unscented KF (UKF) [14] are used.

The step by step operation of the KF is shown in Algorithm~2.

D. Particle Filter

The PF is a recursive sequential Monte Carlo estimation algorithm. The PF approximates the posterior probability density function (PDF) of the state vector with random samples, called particles and updates it iteratively as new information (observation) is received. The estimation accuracy is directly proportional to number of particles N_s . PF does not require the observation model to be linear nor the noise to be Gaussian.

The recursive Bayesian formula to obtain the posterior PDF $p(\mathbf{v}_{1:t} | \mathbf{b}_{1:t})$ from $p(\mathbf{v}_{1:t-1} | \mathbf{b}_{1:t-1})$ is given by

$$p(\mathbf{v}_{1:t} | \mathbf{b}_{1:t}) = \frac{p(\mathbf{b}_t | \mathbf{v}_t) p(\mathbf{v}_t | \mathbf{v}_{t-1})}{p(\mathbf{b}_t | \mathbf{b}_{1:t-1})} p(\mathbf{v}_{1:t-1} | \mathbf{b}_{1:t-1}), \quad (35)$$

where $\mathbf{b}_{1:t}$ is the set of observation from time step 1 to time step t . The posterior PDF is approximated by a set of N_s weighted particles.

$$p(\mathbf{v}_t | \mathbf{b}_t) = \sum_{j=1}^{N_s} w_t^j \delta(\mathbf{v}_t - \mathbf{v}_t^j), \quad (36)$$

where \mathbf{v}_t^j and w_t^j are the particles and weights, respectively. These particles are generated from the proposal density $f(\mathbf{v}_t | \mathbf{b}_t)$ and the weights are given by

$$w_t^j = \frac{p(\mathbf{v}_t^j | \mathbf{b}_t)}{f(\mathbf{v}_t^j | \mathbf{b}_t)}. \quad (37)$$

The proposal density is chosen as

$$f(\mathbf{v}_t | \mathbf{b}_t) = f(\mathbf{v}_t | v_{t-1}, \mathbf{b}_t) f(v_{t-1} | \mathbf{b}_{t-1}). \quad (38)$$

From (35), (37) and (38) we have

$$w_t^j \propto \frac{p(\mathbf{b}_t | \mathbf{v}_t^j) p(\mathbf{v}_t^j | \mathbf{v}_{t-1}^j)}{f(\mathbf{v}_t^j | \mathbf{v}_{t-1}^j, \mathbf{b}_t)} w_{t-1}^j. \quad (39)$$

If the prior $p(v_t | v_{t-1})$ is selected as proposal density then (39) is reduced to

$$w_t^j \propto p(\mathbf{b}_t | \mathbf{v}_t^j) w_{t-1}^j. \quad (40)$$

The marginalized density $p(\mathbf{v}_t | \mathbf{b}_{1:t})$ is given by

$$p(\mathbf{v}_t | \mathbf{b}_t) = \sum_{j=1}^{N_s} w_t^j \delta(\mathbf{v}_t - \mathbf{v}_t^j), \quad (41)$$

which gives us the state vector at time step t .

PF faces degeneracy problem in which most of the particles are given negligible weights. As a results only a few particles are available to approximate the posterior PDF. In order to avoid degeneracy, a resampling technique is used. If the

number of effective particles N_{eff} given by (42) drops below a certain threshold N_{thr} , resampling selects N_s particles from the current particles with repetition, such that particles with higher weights are selected more frequently than the particles with lower weights. These particles replace the current set of particles and all weights are equated to $1/N_s$.

$$N_{eff} = \frac{1}{\sum_{j=1}^{N_s} (w_t^j)^2}. \quad (42)$$

The step by step operation of the PF is shown in algorithm 3.

V. PLE ESTIMATION

In this section, we propose a novel approach that estimate the PLEs for all links, at every time step, in a dynamic environment. For the observation vector $\hat{\mathbf{b}}$ in (9), the cost function, for unknown PLE vector is given by

$$\Omega(\mathbf{u}, \boldsymbol{\alpha}) = \|\mathbf{A}\mathbf{u} - \mathbf{b}\|^2, \quad (43)$$

where $\boldsymbol{\alpha}$ is the unknown PLE vector given by, $\boldsymbol{\alpha} = [\alpha_1, \dots, \alpha_N]^T$. The linear least squares (LLS) solution of \mathbf{u} is given by $\mathbf{u} = \mathbf{A}^\dagger \mathbf{b}$. After replacing it in (43) we obtain

$$\Omega(\boldsymbol{\alpha}) = \left[[\mathbf{b}_x \ \mathbf{b}_y] (\mathbf{I}_{2N} - \mathbf{A}\mathbf{A}^\dagger) [\mathbf{b}_x \ \mathbf{b}_y]^T \right], \quad (44)$$

where $\mathbf{b}_x = \left[\exp\left(\frac{\hat{z}_1}{\gamma\alpha_1}\right) \cos \hat{\theta}_1 \delta_1, \dots, \exp\left(\frac{\hat{z}_N}{\gamma\alpha_N}\right) \cos \hat{\theta}_N \delta_N \right]^T$ and $\mathbf{b}_y = \left[\exp\left(\frac{\hat{z}_1}{\gamma\alpha_1}\right) \sin \hat{\theta}_1 \delta_1, \dots, \exp\left(\frac{\hat{z}_N}{\gamma\alpha_N}\right) \sin \hat{\theta}_N \delta_N \right]^T$ and \mathbf{I}_{2N} is an identity matrix of dimension $2N$. Equation (44) now consists of only one unknown vector i.e., $\boldsymbol{\alpha}$. Solution to which is obtained as follows

$$\hat{\boldsymbol{\alpha}} = \arg \min_{\boldsymbol{\alpha}} \{\Omega(\boldsymbol{\alpha})\}. \quad (45)$$

Equation (45) is a N dimensional optimization problem, which can be solved by conventional *brute force* method. However, it has a high computational cost especially for large number of SNs. To avoid this cost, in this paper we minimize (44) by the generalized pattern search (GenPS) technique [15] which is described in the following sub-section.

A. Generalized Pattern Search

Here we briefly describe the GenPS method in the context of PLE estimation. GenPS belongs to the family of the direct search or derivative-free optimization techniques originally proposed in [15]. Initializing from an initial bounded guess $\boldsymbol{\alpha}_0 \in [2 \ 5]$ and an initial step size $\Delta_0 > 0$, the GenPS iteratively updates the $\boldsymbol{\alpha}^k$ such that $\Omega(\boldsymbol{\alpha}^{k+1}) < \Omega(\boldsymbol{\alpha}^k)$. Each update evaluates the cost function at a point on the mesh \mathcal{M}_k with the updated mesh point closer to the minimum of $\Omega(\boldsymbol{\alpha})$. The iterated steps could operate as a SEARCH (optional) or POLL step. The mesh centered at $\boldsymbol{\alpha}^k$ is defined as follows

$$\mathcal{M}_k = \{\boldsymbol{\alpha}^k + \Delta_k \mathbf{D}\mathbf{z} : \mathbf{z} \in \mathbb{Z}^q\}, \quad (46)$$

$$\mathbf{C}_t(x)_{ii} = \frac{d_{it}^2}{2} \exp\left(\frac{\sigma_{n_i}^2}{(\gamma\alpha_{it})^2} + \sigma_{m_i}^2\right) + \frac{d_{it}^2}{2} \cos(2\theta_{it}) \exp\left(\frac{\sigma_{n_i}^2}{(\gamma\alpha_{it})^2} - \sigma_{m_i}^2\right) - (d_{it} \cos \theta_{it})^2 \quad (32)$$

$$\mathbf{C}_t(y)_{ii} = \frac{d_{it}^2}{2} \exp\left(\frac{\sigma_{n_i}^2}{(\gamma\alpha_{it})^2} + \sigma_{m_i}^2\right) - \frac{d_{it}^2}{2} \cos(2\theta_{it}) \exp\left(\frac{\sigma_{n_i}^2}{(\gamma\alpha_{it})^2} - \sigma_{m_i}^2\right) - (d_{it} \sin \theta_{it})^2 \quad (33)$$

$$\mathbf{C}_t(xy)_{ii} = d_{it}^2 \cos \theta_{it} \sin \theta_{it} \left[\exp\left(\frac{\sigma_{n_i}^2}{(\gamma\alpha_{it})^2} - \sigma_{m_i}^2\right) - 1 \right] \quad (34)$$

$$\mathbf{C}_t(x)_{ij} = 0, \quad \mathbf{C}_t(y)_{ij} = 0, \quad \mathbf{C}_t(xy)_{ij} = 0$$

Algorithm 1 : Initialization and GenPS

for time step $t = 1, \dots$
 for $i = 1, \dots, N$
 estimate the path-loss \hat{z}_i^t and the AoA $\hat{\theta}_i^t$.
 end
 for $k = 1, \dots$
 i. Initialize $\alpha_0 \in [2.5], \Delta_0, \tau, \xi, \nu$.
 ii. Evaluate cost function with all poll points from poll set $\{\alpha^k + \Delta_k \bar{d}, \bar{d} \in \mathbf{D}\}$.
 iii-a. If improved poll point is found, accept α^{k+1} , set $\Delta_{k+1} = \xi \Delta_k$.
 iii-b. If improved poll point cannot be found, set $\alpha^{k+1} = \alpha^k$, set $\Delta_{k+1} = \frac{\Delta_k}{\xi}$.
 Repeat until $\Omega(\alpha^{k+1}) - \Omega(\alpha^k) < \tau$.
 end
 Goto algorithm 2 or algorithm 3.
 end

where $\mathbf{D} \in \mathbb{R}^n$ is a matrix whose columns positively span \mathbb{R}^n , q is the cardinality of \mathbf{D} . Also \mathbf{D} must be a product $\mathbf{D} = \mathbf{G}\mathbf{Z}$, where $\mathbf{G} \in \mathbb{R}^n$ and is non singular while $\mathbf{Z} \in \mathbb{Z}^{n \times q}$. For the present problem, we have $\mathbf{G} = \frac{1}{\nu} \mathbf{I}_N$ where $\nu > 1$ and represents the precision of the mesh. At the k^{th} POLL, the objective function is evaluated at neighboring poll points given by

$$\text{Poll points} = \{\alpha^k + \Delta_k \bar{d}, \bar{d} \in \mathbf{D}\}. \quad (47)$$

If the evaluation of the cost function at any of the poll points during the k^{th} iterations decreases its value then the poll α^{k+1} , is accepted and the length of the step size is increased $\Delta_{k+1} = \xi \Delta_k$ for any scalar $\xi > 1$. Otherwise if the poll is rejected then $\alpha^{k+1} = \alpha^k$ while the length of the step size is reduced by the same factor i.e., $\Delta_{k+1} = \frac{\Delta_k}{\xi}$. The algorithm is repeated until a stopping condition is reached e.g., $\Omega(\alpha^{k+1}) - \Omega(\alpha^k) < \tau$, where τ is some small value.

By exploiting the GenPS technique, the computational load significantly decreases and (44) is minimized with a few iterations. Once the estimated PLEs are available, they are used to update (26) which in turn serves as the updated observation for KF or PF for tracking of the TN. The step by step procedure for tracking using estimated PLEs is shown in algorithms 1, 2 and 3.

Algorithm 2 : Kalman Filter

Generate initial state \mathbf{v}_0 and initial Covariance matrix \mathbf{W}_0 .

i. Prediction.

Predict $\bar{\mathbf{v}}_t$ by propagating \mathbf{v}_0 through the motion model.

$$\bar{\mathbf{v}}_t = \mathbf{S} \hat{\mathbf{v}}_{t-1} + \mathbf{r}_t$$

Predict $\bar{\mathbf{W}}_t$ by

$$\bar{\mathbf{W}}_t = \mathbf{S} \mathbf{W}_{t-1} \mathbf{S}^T + \mathbf{Q}$$

ii. Measurement update

Estimate Kalman gain

$$\mathbf{K}_t = \bar{\mathbf{W}}_t \mathbf{H}^T (\mathbf{H} \bar{\mathbf{W}}_t \mathbf{H}^T + \mathbf{C})$$

Update the predicted state vector and predicted error covariance matrix.

$$\hat{\mathbf{v}}_t = \bar{\mathbf{v}}_t + \mathbf{K}_t (\hat{\mathbf{b}}_t - \mathbf{H} \bar{\mathbf{p}}_t)$$

$$\mathbf{W}_t = (\mathbf{I}_4 - \mathbf{K}_t \mathbf{H}) \bar{\mathbf{W}}_t$$

Set $t = t + 1$. Go to Algorithm 1.

VI. SIMULATION RESULTS

We consider a fully connected 2-dimensional network of 150m \times 150m with a single TN, with unknown velocity, direction and coordinates. We also consider N SNs at the boundary of the network. All simulations are run ϵ times independently.

In Fig.1, the theoretical root-MSE (RMSE) and simulation RMSE of location estimates are compared in a scenario for erroneous PLE values. For simplicity only two SNs are considered. Two different values i.e., $\alpha_1 = 2.5$ and $\alpha_2 = 3$ are considered for each SN-TN link. The error $e_1 = \check{\alpha}_1 - \alpha_1$ and $e_2 = \check{\alpha}_2 - \alpha_2$ in the PLEs are shown in the x and y coordinates in the figure while the z coordinates represents the RMSE in location estimate. The shadowing variance is $\sigma_{n_i}^2 = 1$ dB $\forall i$ while the error in angle estimates is $\sigma_{m_i}^2 = 1^0 \forall i$. The simulation results are averaged over $\epsilon = 500$ independent runs. It is clear from the plot that even a small error in PLEs has a significant impact on localization accuracy. It is also seen that incorrect PLE assumptions that are underestimated have a greater impact on location inaccuracy than overestimated values. Furthermore, it is evident from Fig. 1 that the theoretical MSE accurately predicts the system performance.

Fig. 2 shows the true trajectory of TN motion and per-

Algorithm 3 : Particle Filter

Initialization:

Generate samples $\{v_0^{j*} \sim \mathcal{N}(\mu_0, \sigma_0^2)\}$, $j = 1, \dots, N_s$. Set

$$w_0^j = \frac{1}{N_s}.$$

i. Prediction:

For $j = 1, \dots, N_s$, predict according to

$$v_t^j = p(v_t | v_{t-1}^{j*})$$

ii. Weight update

Update the weights according to

$$w_t^j = p(\mathbf{b}_t | v_t^j) w_{t-1}^j$$

Normalize weights by

$$\tilde{w}_t^j = \frac{w_t^j}{\sum_{j=1}^{N_s} w_t^j}$$

iii. Estimate Output

The state is estimated by the mean of posterior i.e

$$\hat{v}_t = E[p(v_t | \mathbf{b}_t)]$$

or

$$\hat{v}_t = \frac{1}{N_s} \sum_{j=1}^{N_s} \tilde{w}_t^j v_t^j$$

resample if required. Set $t = t + 1$ and $w_t^j = \frac{1}{N_s}$. Go to algorithm 1.

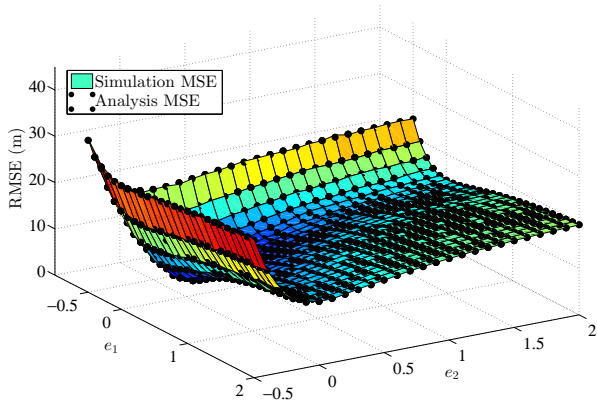


Fig. 1. Performance comparison between simulation and analytical MSE. $TN = [36 \ 19]^T$, $SNs = [0 \ 0 \ 0 \ 50]^T$, $e_i = \tilde{\alpha}_i - \alpha_i$, $\alpha_1 = 2.5$, $\alpha_2 = 3$, $N = 2$, $\sigma_{n_i}^2 = 1 \text{ dB} \forall i$, $\sigma_{m_i}^2 = 1^0 \forall i$, $\epsilon = 500$.

formance comparison of tracking via KF for erroneous PLE values and estimated PLEs. The true values of the PLEs are considered to be changing at every time step and drawn randomly from a uniform distribution i.e., $\alpha \in \mathcal{U}[2 \ 5]$. The erroneous PLEs are generated by adding a random noise with a Gaussian distribution of variance σ_α^2 and mean zero at every time step. However, it is assumed that the realization of the added noise does not change within each time step. For Fig. 2, $\sigma_\alpha^2 = 0.2$. The estimated angle and the shadowing variance is kept fixed at $\sigma_{m_i}^2 = 5^0$ and $\sigma_{n_i}^2 = 5 \text{ dB} \forall i$ respectively.

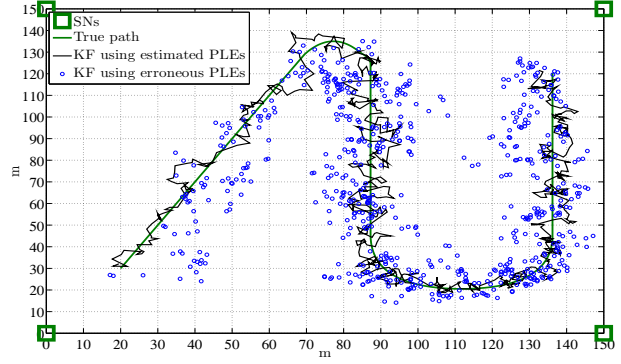


Fig. 2. Performance comparison of KF using erroneous PLEs and estimated PLEs. $T_s = 1 \text{ sec}$, $\sigma_{m_i}^2 = 5^0 \forall i$, $\sigma_{n_i}^2 = 5 \text{ dB} \forall i$, $\alpha \in \mathcal{U}[2 \ 5]$, $\sigma_\alpha^2 = 0.2$, $\epsilon = 1$, $\Delta_0 = 0.1$, $v = 10$, $\xi = 2$, $\tau = 3$, $\epsilon = 1$, $N = 4$.

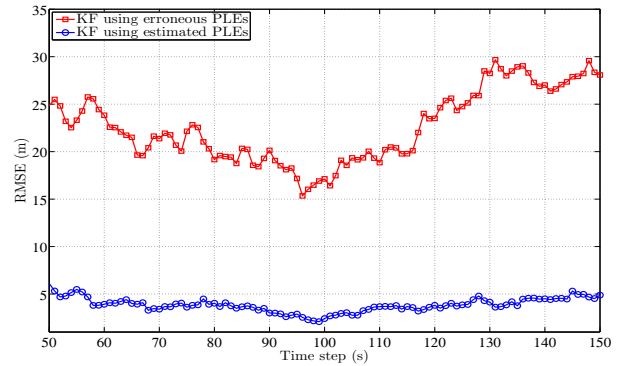


Fig. 3. RMSE comparison of tracking via KF using estimated and erroneous PLE values. $T_s = 1 \text{ sec}$, $\sigma_{m_i}^2 = 5^0 \forall i$, $\sigma_{n_i}^2 = 5 \text{ dB} \forall i$, $\alpha \in \mathcal{U}[2 \ 5]$, $\sigma_\alpha^2 = 0.5$, $\Delta_0 = 0.1$, $v = 10$, $\xi = 2$, $\tau = 3$, $\epsilon = 30$, $N = 4$.

The GenPS algorithm estimates the PLEs before the filtering process at every time step of $T_s = 1 \text{ s}$, the parameters of the GenPS algorithm are given at the bottom of Fig. 2. It is evident from the trajectories in Fig. 2 that KF with PLE estimation via GenPS performs considerably better than the KF with incorrectly assumed PLEs.

Fig. 3 keeps the same parameters as in Fig. 2 and compares the RMSE at every time step using KF with an erroneous and estimated PLE vector. The RMSE values are an average over $\epsilon = 30$ independent runs. Fig. 3 presents a quantitative comparison of KF performance with erroneous and estimated PLEs. The significant performance improvement of KF with estimated PLEs is evident from the figure.

Fig. 4 shows the true trajectory of the motion of the TN, the estimated trajectory with PF using erroneous PLEs and the trajectory of the PF with estimated PLEs. The estimated angle and the shadowing variance is kept fixed at $\sigma_{m_i}^2 = 5^0 \forall i$ and $\sigma_{n_i}^2 = 5 \text{ dB} \forall i$ respectively. Similar to Fig. 2 and Fig. 3, $\alpha \sim \mathcal{U}[2 \ 5]$ and $\tilde{\alpha} \sim \mathcal{U}[2 \ 5]$. For the PF, we consider $N_s = 2000$ particles. Following the pattern set by the KF in Fig. 2, the PF with PLE estimation exhibits superior performance to the same with erroneous PLEs.

Keeping the parameters the same as in Fig. 4, Fig. 5

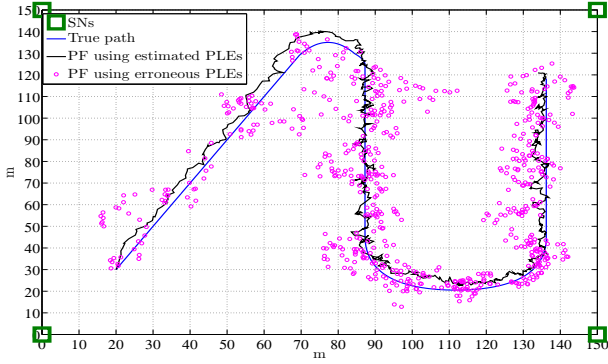


Fig. 4. Performance comparison of tracking via PF while using erroneous and estimated PLE values. $T_s = 1$ sec, $N_s = 2000$, $N_{thr} = N_s/4$, $\sigma_{m_i}^2 = 5^0 \forall i$, $\sigma_{n_i}^2 = 5$ dB $\forall i$, $\alpha \in \mathcal{U}[2, 5]$, $\sigma_\alpha^2 = 0.2$, $\Delta_0 = 0.1$, $v = 10$, $\xi = 2$, $\tau = 3$, $\epsilon = 1$.

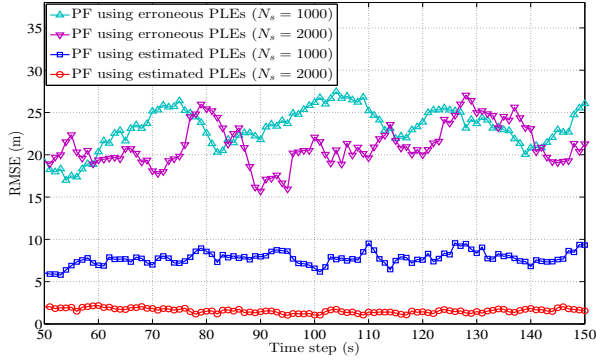


Fig. 5. RMSE in location estimate utilizing PF, using estimated and erroneous PLE values. $T_s = 1$ sec, $\sigma_{m_i}^2 = 5^0 \forall i$, $\sigma_{n_i}^2 = 5$ dB $\forall i$, $N_{thr} = N_s/10$, $\alpha \in \mathcal{U}[2, 5]$, $\sigma_\alpha^2 = 0.5$, $\Delta_0 = 0.1$, $v = 10$, $\xi = 2$, $\tau = 3$, $\epsilon = 30$.

compares the RMSE between of the PF with and without PLE estimation. The simulations are run $\epsilon = 30$ times. For both cases, two different sets of particles i.e., $N_s = 1000$ and $N_s = 2000$ are used. It is seen that the performance of PF with incorrect PLEs does not vary with different N_s values, this is because the incorrect PLEs induces such a large error in the observation vector that the PF does not converge even with a large numbers of particles. On the other hand, it is seen that while estimating the PLEs with GenPS, considerable performance improvement is achieved with an increased number of particles.

In Fig. 6 we compare the performance of both KF and PF using GenPS for PLE estimation. Two different values of the number of particles i.e., $N_s = 1000$, and 2000 are taken for PF tracking. Also two sets of shadowing variance and angle noise variance i.e., $\sigma_n^2 = 5$ dB, $\sigma_m^2 = 5^0$ and $\sigma_n^2 = 10$ dB, $\sigma_m^2 = 10^0$ are considered for both KF and PF. In both scenarios the PF performs better than the KF. The reason behind this improved performance of the PF over KF is the non-Gaussian distribution of the observation vector $\hat{\mathbf{b}}$.

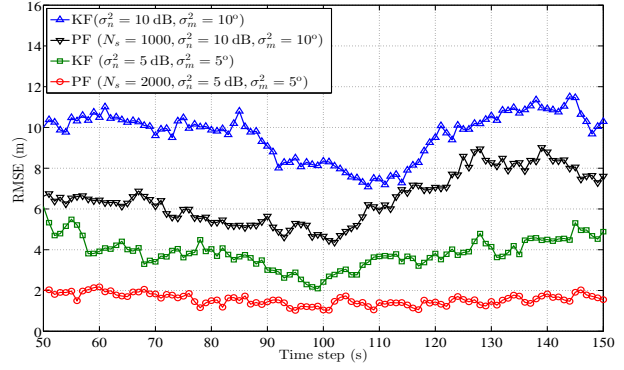


Fig. 6. Performance comparison between PF and KF using estimated PLE. $T_s = 1$ sec, $N_{thr} = N_s/10$, $N_{thr} = N_s/10$, $\alpha \in \mathcal{U}[2, 5]$, $\sigma_\alpha^2 = 0.5$, $\Delta_0 = 0.1$, $v = 10$, $\xi = 2$, $\tau = 3$, $\epsilon = 30$.

VII. CONCLUSION

In this paper we presented a novel online algorithm for joint PLE and tracking when both distance and bearing measurements are available. First, a closed form expression MSE is derived to highlight the impact of incorrectly assumed PLEs on location estimation. Second, the GenPS algorithm is used to estimate dynamic PLEs for every SN-TN link at each time step. Once the PLEs are estimated they are used in both KF and PF for tracking. In the simulation section, we showed that the tracking performance degrades when the PLE values is incorrect. The performance can be considerably improved when the PLEs are estimated online.

ACKNOWLEDGMENT

We acknowledge the support from the UK Engineering and Physical Sciences Research Council (EPSRC) for the support via the Bayesian Tracking and Reasoning over Time (BTaRoT) grant EP/K021516/1.

APPENDIX

The submatrices in (16) are given by

$$\mathbf{C}_\alpha(x) = E_{n,m} \left[\left(\hat{\mathbf{b}}_x - \mathbf{b}_x \right) \left(\hat{\mathbf{b}}_x - \mathbf{b}_x \right)^T \right] \quad (48)$$

$$\mathbf{C}_\alpha(y) = E_{n,m} \left[\left(\hat{\mathbf{b}}_y - \mathbf{b}_y \right) \left(\hat{\mathbf{b}}_y - \mathbf{b}_y \right)^T \right] \quad (49)$$

$$\mathbf{C}_\alpha(xy) = E_{n,m} \left[\left(\hat{\mathbf{b}}_x - \mathbf{b}_x \right) \left(\hat{\mathbf{b}}_y - \mathbf{b}_y \right)^T \right] \quad (50)$$

for $\hat{\mathbf{b}}_x = \left[d_1^{\beta_1} \exp\left(\frac{n_1}{\gamma\alpha_1}\right) \cos \hat{\theta}_1 \delta_1, \dots, d_N^{\beta_N} \exp\left(\frac{n_N}{\gamma\alpha_N}\right) \cos \hat{\theta}_N \delta_N \right]^T$
and $\hat{\mathbf{b}}_y = \left[d_1^{\beta_1} \exp\left(\frac{n_1}{\gamma\alpha_1}\right) \cos \hat{\theta}_1 \delta_1, \dots, d_N^{\beta_N} \exp\left(\frac{n_N}{\gamma\alpha_N}\right) \cos \hat{\theta}_N \delta_N \right]^T$.

Proof of (17): For the diagonal terms i.e $i = j$, putting value in (48)

$$\begin{aligned}
\mathbf{C}(x)_{ii} &= E_{n_i, m_i} \left[\left(d_i^{\beta_i} \exp\left(\frac{n_i}{\gamma \check{\alpha}_i}\right) \cos(\theta_i + m_i) \check{\delta}_i - d_i \cos \theta_i \right)^2 \right], \\
&= E_{n_i, m_i} \left[d_i^{2\beta_i} \exp\left(\frac{2n_i}{\gamma \check{\alpha}_i}\right) \cos^2(\theta_i + m_i) \check{\delta}_i^2 + \left(d_i \cos \theta_i \right)^2 \right. \\
&\quad \left. - 2\check{\delta}_i \left(d_i \cos \theta_i \right) \left(d_i^{\beta_i} \exp\left(\frac{n_i}{\gamma \check{\alpha}_i}\right) \right) \cos(\theta_i + m_i) \right], \tag{51}
\end{aligned}$$

$$\begin{aligned}
\mathbf{C}(x)_{ii} &= E_{n_i, m_i} \left[d_i^{2\beta_i} \exp\left(\frac{2n_i}{\gamma \check{\alpha}_i}\right) \left(\frac{1}{2} + \frac{1}{2} \cos(2\theta_i + 2m_i) \right) \check{\delta}_i^2 \right. \\
&\quad \left. + \left(d_i \cos \theta_i \right)^2 - 2\check{\delta}_i d_i d_i^{\beta_i} \exp\left(\frac{n_i}{\gamma \check{\alpha}_i}\right) \cos(\theta_i + m_i) \cos \theta_i \right] \tag{52}
\end{aligned}$$

Equation (52) is obtained from (51) by using trigonometric half angle identity, $\cos^2(t) = 0.5 + 0.5 \cos(2t)$. Also using trigonometric sum-difference formula, $\cos(a+b) = \cos a \cos b + \sin a \sin b$, (53) is obtained

$$\begin{aligned}
\mathbf{C}(x)_{ii} &= E_{n_i, m_i} \left[d_i^{2\beta_i} \exp\left(\frac{2n_i}{\gamma \check{\alpha}_i}\right) \left(\frac{1}{2} + \frac{1}{2} (\cos 2\theta_i \cos 2m_i \right. \right. \\
&\quad \left. \left. + \sin 2\theta_i \sin 2m_i) \right) \check{\delta}_i^2 + \left(d_i \cos \theta_i \right)^2 - 2\check{\delta}_i d_i d_i^{\beta_i} \exp\left(\frac{n_i}{\gamma \check{\alpha}_i}\right) \right. \\
&\quad \left. (\cos^2 \theta_i \cos m_i + \sin \theta_i \sin m_i) \right] \tag{53}
\end{aligned}$$

Finally, using expectations

$$E_{m_i}[\cos(m_i)] = \exp(-0.5\sigma_{m_i}^2), \quad E_{m_i}[\cos(2m_i)] = \exp(-2\sigma_{m_i}^2) \tag{54}$$

$$E_{m_i}[\sin(m_i)] = 0, \quad E_{m_i}[\sin(2m_i)] = 0 \tag{55}$$

$$\begin{aligned}
E_{n_i} \left[\exp\left(\frac{n_i}{\gamma \check{\alpha}}\right) \right] &= \exp\left(\frac{\sigma_{n_i}^2}{2(\gamma \check{\alpha})^2}\right), \\
E_{n_i} \left[\exp\left(\frac{2n_i}{\gamma \check{\alpha}}\right) \right] &= \exp\left(\frac{2\sigma_{n_i}^2}{(\gamma \check{\alpha})^2}\right) \tag{56}
\end{aligned}$$

we conclude the proof by obtaining (17).

The proof of (18) and (19) is similar to (17) except for the fact that $\hat{\mathbf{b}}_x$ is replaced by $\hat{\mathbf{b}}_y$.

Proof of (20) : For the non-diagonal terms i.e $i \neq j$, putting values of $\hat{\mathbf{b}}_x$ and $\hat{\mathbf{b}}_y$ in (48)

$$\begin{aligned}
\mathbf{C}(x)_{ij} &= E_{n_i, m_i} \left[\left\{ d_i^{\beta_i} \exp\left(\frac{n_i}{\gamma \check{\alpha}_i}\right) \cos(\theta_i + m_i) \check{\delta}_i - d_i \cos \theta_i \right\} \right. \\
&\quad \left. \left\{ d_j^{\beta_j} \exp\left(\frac{n_j}{\gamma \check{\alpha}_j}\right) \cos(\theta_j + m_j) \check{\delta}_j - d_j \cos \theta_j \right\} \right] \tag{57}
\end{aligned}$$

$$\begin{aligned}
\mathbf{C}(x)_{ij} &= d_i^{\beta_i} d_j^{\beta_j} \exp\left(\frac{n_i}{\gamma \check{\alpha}_i} + \frac{n_j}{\gamma \check{\alpha}_j}\right) \left(\cos \theta_i \cos m_i \cos \theta_j \cos m_j \right. \\
&\quad \left. + \cos \theta_i \cos m_i \sin \theta_j \sin m_j + \sin \theta_i \sin m_i \cos \theta_j \cos m_j \right. \\
&\quad \left. + \sin \theta_i \sin m_i \sin \theta_j \sin m_j \right) \check{\delta}_i \check{\delta}_j - d_i^{\beta_i} d_j \exp\left(\frac{n_i}{\gamma \check{\alpha}_i}\right) \\
&\quad \cos \theta_i \cos m_i \cos \theta_j \check{\delta}_i - d_j^{\beta_j} d_i \exp\left(\frac{n_j}{\gamma \check{\alpha}_j}\right) \cos \theta_j \\
&\quad \cos m_j \cos \theta_i \check{\delta}_j + d_i d_j \cos \theta_i \cos \theta_j. \tag{58}
\end{aligned}$$

Equation (58) is obtained using (57) using half angle identity and sum-difference formula. Finally using expectation given by (54), (55) and (56) we obtain (20).

The proof of (21) and (22) is similar to the other proofs except for the fact that $\hat{\mathbf{b}}_x$ is replaced by $\hat{\mathbf{b}}_y$.

REFERENCES

- [1] S. Haykin, *Communication Systems*, 5th ed. Wiley Publishing, 2009.
- [2] N. Salman, A. H. Kemp, and M. Ghogho, "Low complexity joint estimation of location and path-loss exponent," *IEEE Wireless Communications Letters.*, vol. 1, no. 4, pp. 364–367, 2012.
- [3] N. Salman, Y. J. Guo, A. H. Kemp, and M. Ghogho, "Analysis of linear least square solution for RSS based localization," in *International Symposium on Communications and Information Technologies (ISCIT)*, Oct 2012, pp. 1051–1054.
- [4] X. Li, "RSS-based location estimation with unknown pathloss model," *IEEE Transactions on Wireless Communications.*, vol. 5, no. 12, pp. 3626–3633, 2006.
- [5] N. Salman, M. W. Khan, and A. H. Kemp, "Enhanced hybrid positioning in wireless networks II: AoA-RSS," in *International Conference on Telecommunications and Multimedia (TEMU)*, July 2014, pp. 92–97.
- [6] A. Nasipuri and K. Li, "A directionality based location discovery scheme for wireless sensor networks," in *Proceedings of the 1st ACM International Workshop on Wireless Sensor Networks and Applications*. ACM, 2002, pp. 105–111.
- [7] P. Kulakowski, J. Vales-Alonso, E. Egea-López, W. Ludwin, and J. Garcia-Haro, "Angle-of-arrival localization based on antenna arrays for wireless sensor networks," *Computers & Electrical Engineering*, vol. 36, no. 6, pp. 1181 – 1186, 2010.
- [8] R. Schmidt, "Multiple emitter location and signal parameter estimation," *IEEE Transactions on Antennas and Propagation.*, vol. 34, no. 3, pp. 276–280, 1986.
- [9] R. Roy and T. Kailath, "ESPRIT-estimation of signal parameters via rotational invariance techniques," *IEEE Transactions on Acoustics, Speech and Signal Processing.*, vol. 37, no. 7, pp. 984–995, 1989.
- [10] R. E. Kalman, "A new approach to linear filtering and prediction problems," *Transactions of the ASME–Journal of Basic Engineering*, vol. 82, no. Series D, pp. 35–45, 1960.
- [11] L. Mihaylova and A. Carmi, "Particle algorithms for filtering in high dimensional state spaces: A case study in group object tracking," in *IEEE International Conference on Acoustics, Speech and Signal Processing (ICASSP) 2011.*, May 2011, pp. 5932–5935.
- [12] S. M. Kay, *Fundamentals of Statistical Signal Processing: Estimation Theory*. Upper Saddle River, NJ: Prentice Hall, Inc., 1993.
- [13] T. Camp, J. Boleng, and V. Davies, "A survey of mobility models for ad hoc network research," *Wireless Communications and Mobile Computing*, vol. 2, no. 5, pp. 483–502, 2002.
- [14] S. Julier and J. Uhlmann, "Unscented filtering and nonlinear estimation," *Proceedings of the IEEE*, vol. 92, no. 3, pp. 401–422, Mar 2004.
- [15] V. Torczon, "On the convergence of pattern search algorithms," *SIAM J. on Optimization*, vol. 7, no. 1, pp. 1–25, Jan. 1997.